ELSEVIER

Polymer 42 (2001) 2637–2645

polymer

www.elsevier.nl/locate/polymer

Crystallization and melting behaviour of poly(butylene naphthalene-2,6-dicarboxylate)

G.Z. Papageorgiou, G.P. Karayannidis*

Laboratory of Organic Chemical Technology, Department of Chemistry, Aristotle University of Thessaloniki, GR-540 06, Thessaloniki, Macedonia, Greece

Received 12 June 2000; received in revised form 20 July 2000; accepted 25 August 2000

Abstract

Isothermal crystallization of poly(butylene naphthalene-2,6-dicarboxylate) (PBN), from the melt, at various crystallization temperatures ranging from 213 up to 225°C was studied. During isothermal crystallization, relatively high crystallinity was found to develop. Isothermal crystallization kinetics was studied using the Avrami equation. For non-isothermal studies, PBN was crystallized by cooling rates ranging from 0.5 to 20°C/min. Only semicrystalline PBN was produced, not depending on the cooling process. The Ozawa and modified-Avrami approaches were used to describe the non-isothermal crystallization kinetics of PBN. Recrystallization phenomena and multiple melting peaks were observed during heating of isothermally and non-isothermally crystallized samples. Annealing at temperatures very close to the original melting point increased the latter from 248 to 264°C.

Keywords: Poly(butylene naphthalene-2,6-dicarboxylate) or poly(butylene 2,6-naphthalate); Poly(ethylene naphthalene-2,6-dicarboxylate); Isothermal crystallization

1. Introduction

Properties of polymeric materials are dependent on the morphology generated during their processing, which is usually non-isothermal. Crystallization of a polymer or even a polymer matrix in composites may cause a volume reduction up to 20%, which in turn results in generation of mechanical stresses. So, the knowledge of their crystallization parameters is needed for the optimization of the processing conditions and the properties of the end products [1].

At least first stages of isothermal crystallization, i.e. up to 30% degree of conversion, can be adequately described by the so-called Avrami equation [2–7]. However, non-isothermal crystallization of polymers is quite difficult to be modelled. Some authors tried to model the non-isothermal process, assuming it can be approximated by a sequence of infinitesimally small isothermal stages, so that it can be described by models based on modifications of the Avrami equation [8–24].

Poly(butylene naphthalene-2,6-dicarboxylate), (PBN), (I) is a new polyester, with excellent chemical resistance, as also mechanical, thermal and insulating properties. Especially, PBN fibres can be used in many applications. So, crystallization of PBN during fibre spinning is of great importance.

PBN shows fast crystallization rates compared with other polyesters. The enhanced PBN chain mobility due to the flexibility of the long butylene groups, as well as the interchain interactions due to the naphthalene rings, can give rise to fast nucleation and crystal growth from the melt. So that PBN can not be obtained in the amorphous glassy state by cooling from the melt in contrast to poly(ethylene naphthalene-2,6-dicarboxylate), (PEN) [25].

Melting of PBN [26] has also interest since various metastable crystalline phases are produced during solidification. Recrystallization and annealing are significant phenomena for polymers with enhanced crystallizability.

In this paper, the crystallization of PBN was studied, using both isothermal and non-isothermal crystallization on cooling from the melt. Isothermal crystallization was treated using the Kolmogorov–Mehl–Avrami equation [4–6], while the Ozawa [8] and modified-Avrami approaches [15,22] were elaborated for non-isothermal crystallization. Since PBN can be easily crystallized over a wide range of temperatures and cooling rates, PBN crystallization was studied under various crystallization conditions. Also, the melting of PBN was studied in order to determine the effect of the crystallization conditions on the resulting morphology.

* Corresponding author. Tel.: +30-31-997-814; fax: +30-31-997-769.
E-mail address: karayan@chem.auth.gr (G.P. Karayannidis).

0032-3861/01/$ - see front matter
PII: S0032-3861(00)00640-6

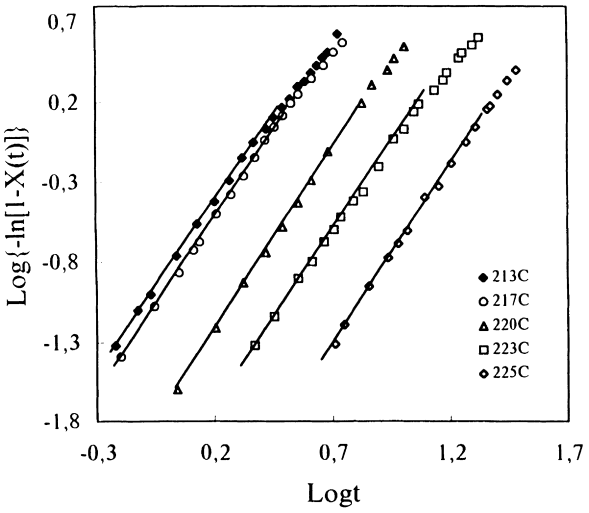

Fig. 1. Avrami plots for isothermal crystallization of PBN from the melt at various temperatures.

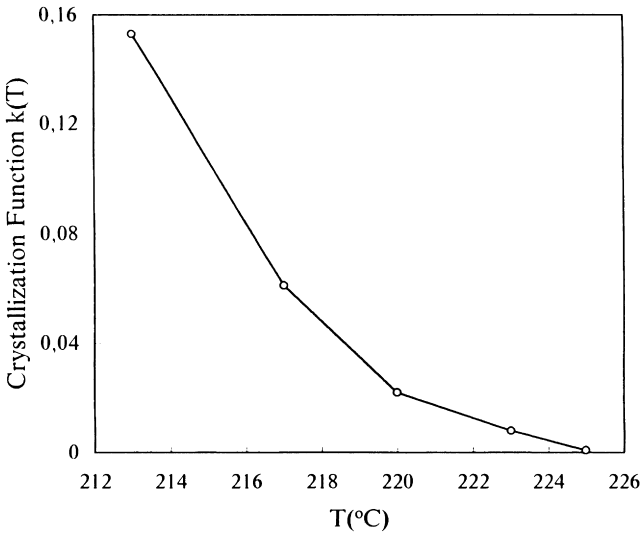

Fig. 2. Dependence of the crystallization growth function k on crystallization temperature *T*, for isothermal crystallization of PBN from the melt.

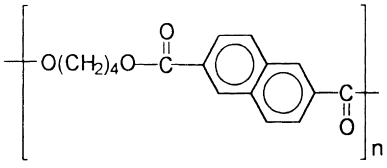

(I)

2. Experimental

PBN was synthesized by polycondensation from dimethyl-naphthalene-2,6-dicarboxylate, (DMN) and 1,4-butane-diol, using $Ti(OBu)_4$ as catalyst. Synthesis was described in details in an our previous paper [27]. The intrinsic viscosity of the resin was found to be 0.61 dl/g in a mixed solvent phenol/tetrachloroethane 60/40% w/w at 25°C.

Crystallizations of PBN were performed in a Perkin–Elmer Pyris 1 differential scanning calorimeter (DSC). Samples of 5 ± 0.01 mg were used. It is important for crystallization experiments to minimize the thermal lag, so samples of less or equal to 5 mg should be used in DSC tests. Isothermal crystallization tests were performed at temperatures from 213 to 225°C. The samples were initially melted at 280°C for 5 min to erase all previous thermal history and then cooled by 150°C/min to the crystallization temperatures. Since crystallization at lower temperatures is very fast, problems could be caused in computations, because crystallization induction time is shorter than the time needed for the instrument to equilibrate, or crystallization may be initiated during cooling.

For non-isothermal crystallizations, samples were cooled at various cooling rates. Crystallizations were performed at cooling rates 0.5, 1, 2.5, 5, 7.5, 10, 15, 20, 30, 40, 50, 60, 80, 100 and 120°C/min, though for quantitative analysis of crystallization only rates up to 20°C/min were used.

In order to study PBN melting, heating scans were performed at various heating rates from 2.5 to 80°C/min. Annealing was also performed at high enough temperatures, where melting of the samples had already started.

Table 1
Avrami exponent and crystallization growth function for isothermal crystallization of PBN

Crystallization temperature T_c (°C)	Avrami exponent n	Crystallization growth function $k(T)$ $(\text{min})^{1/n}$
213	2.21	0.143000
217	2.16	0.060900
220	2.20	0.019950
223	2.34	0.007940
225	2.38	0.000786

3. Results and discussion

3.1. Isothermal crystallization

Isothermal crystallizations were performed at 213, 217, 220, 223 and 225°C. Crystallization exotherms vs crystallization time were recorded. The Avrami equation was used to evaluate the crystallization parameters. In the Avrami equation

$$1 - X(t) = \exp(-kt^n) \quad (1)$$

$X(t)$ is the relative crystallinity; n the Avrami exponent which is a function of the nucleation process; and k the growth function which is dependent on nucleation and

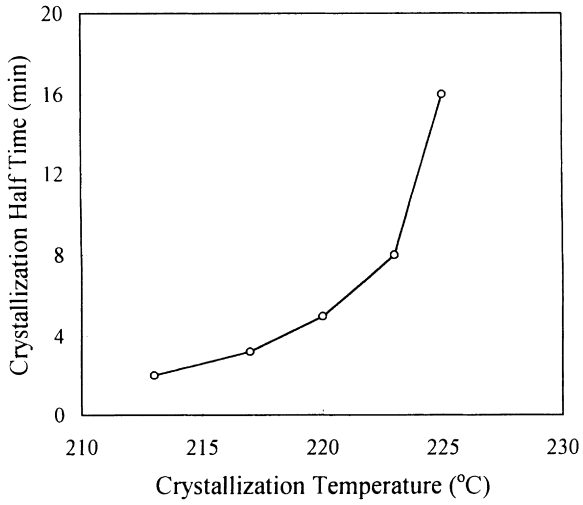

Fig. 3. Crystallization half time $t_{1/2}$ vs crystallization temperature T, for isothermal crystallization of PBN from the melt.

crystal growth. Plots of $\log\{-\ln[1-X(t)]\}$ vs $\log t$ are shown in Fig. 1. From the slope and the intersection, values of n and k, respectively were calculated and the results are summarized in Table 1. The n values found to be between 2.16 and 2.38, which are slightly higher than those reported by Lee et al. [28]. However, Lee et al., performed isothermal crystallizations of PBN at T_cs between 205 and 220°C after melting at 300°C for 15 min and found n values between 2.10 and 2.24.

The plot of $k(T)$ vs T_c is shown in Fig. 2, where one can see that $k(T)$ increase with supercooling. This increase is rather exponential. In Fig. 3 it is shown that crystallization half time $t_{1/2}$ decreases with decreasing crystallization temperature, that is the crystallization rate increases with supercooling.

3.2. Non-isothermal crystallization

For non-isothermal crystallization studies, crystallizations at various cooling rates should be performed. Since PBN can crystallize even during fast cooling a large variety of cooling rates was applied, ranging from 0.5 to 120°C/min (see Section 2) in order to obtain a more clear picture of the phenomenon. In Fig. 4 the S type curves consistent for a nucleation and growth process, represent the dependence of relative crystallinity as a function of temperature, during cooling at constant cooling rate. One can see that as the cooling rate increases, the crystallization temperature range gets wider and it shifts to lower temperatures.

For the analysis of the experimental results the Ozawa approach and two different modified-Avrami approaches were elaborated.

3.2.1. Ozawa analysis of non-isothermal crystallization

According to Ozawa theory [8], the degree of conversion at temperature T, $X(T)$, can be calculated as:

$$-\ln[1-X(T)] = k(T)/\alpha^n$$

where α is the cooling rate, n is the Avrami exponent and k is the cooling crystallization function. k is related to the overall crystallization rate and indicates how fast crystallization occurs. From the Ozawa equation it follows:

$$\log\{-\ln[1-X(T)]\} = \log k(T) - n\log\alpha.$$

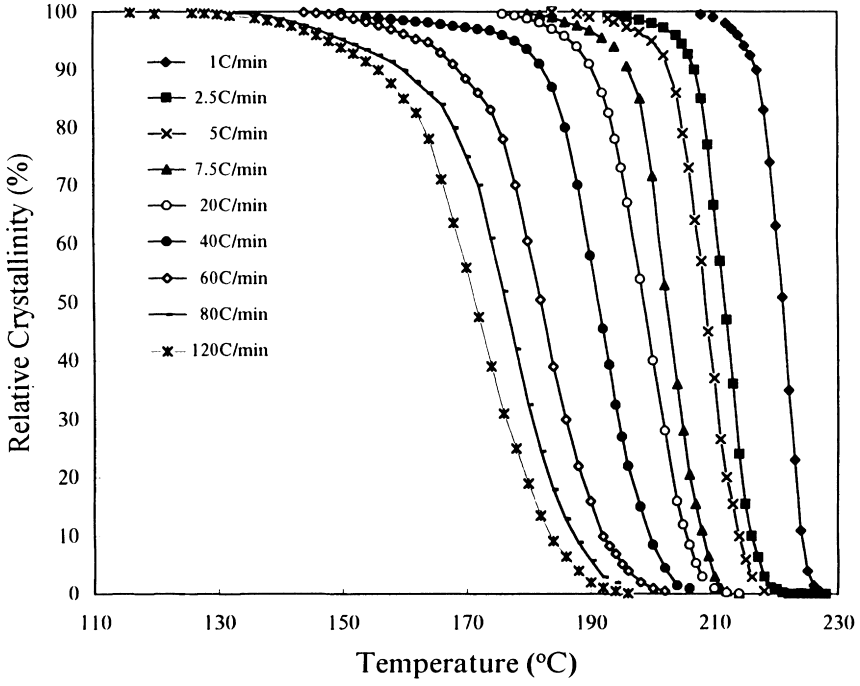

Fig. 4. Relative crystallinity vs temperature for non-isothermal crystallization of PBN at various cooling rates.

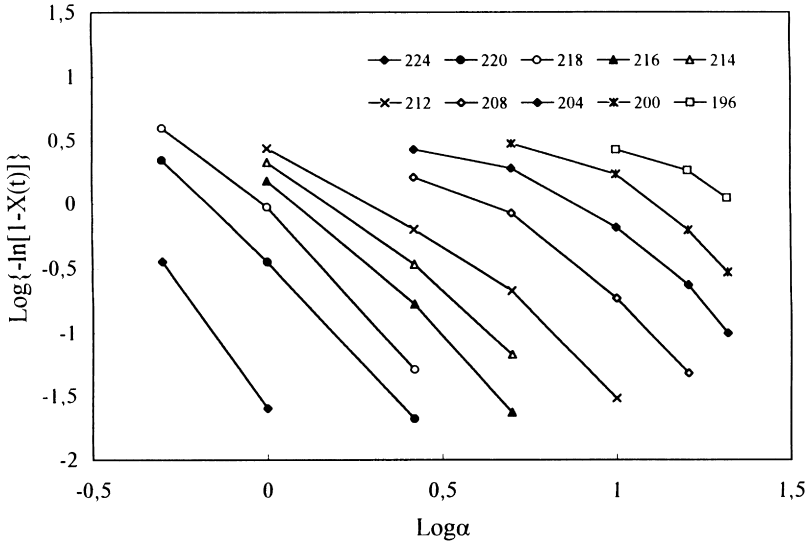

Fig. 5. Ozawa plots for non-isothermal crystallization of PBN.

By plotting $\log\{-\ln[1-X(T)]\}$ vs $\log\alpha$, a straight line should be obtained and the kinetic parameters n and k can be achieved from the slope and the intercept, respectively.

For PBN non-isothermally crystallized by cooling at constant rates from 0.5 to 20°C/min plots, of $\log\{-\ln[1-X(T)]\}$ vs $\log\alpha$ can be seen in Fig. 5. From these plots, one can conclude that linearity does exist at the lower part of the plots, while curvature is observed at the upper part. This is reasonable since the lower part of plots is related with values calculated for the first stages of crystallization, while the upper part is related with later stages during which crystallization is retarted, since it takes place in a constraint environment, i.e. probably related with secondary crystallization. Ozawa, in his approach, ignored secondary crystallization and the dependence of the fold length on temperature [8]. However, Lopez and Wilkes [18] argued that during cooling, secondary crystallization should be absent since temperature is lowered continuously.

Di Lorenzo and Silvestre, in their recent review concluded that the Ozawa method does not describe adequately the non-isothermal crystallization kinetics for polymers like PE, PEEK or Nylon 11 for which a large portion of the overall crystallization is attributed to secondary crystallization.

However, in most of the previous works though some curvature was always more or less present in the Ozawa plots, this was usually ignored. For the case of PBN, if it is assumed that the linearity of the Ozawa plots is good for data from the early stages of crystallization, the n and k values summarized in Table 2 are found. As it can be seen, in Table 2, n was found to increase with temperature from 2.05 (for 196°C) to 3.92 (for 224°C), while an

Table 2
Results from Ozawa analysis of PBN non-isothermal crystallization

Crystallization temperature T_c (°C)	Ozawa exponent n	$\log k(T)$
224	3.92	−1.610
220	2.64	−0.460
218	2.41	−0.050
216	2.35	0.165
214	2.02	0.339
212	2.39	0.474
208	2.11	1.390
204	2.16	2.017
200	2.10	2.380
196	2.05	2.640

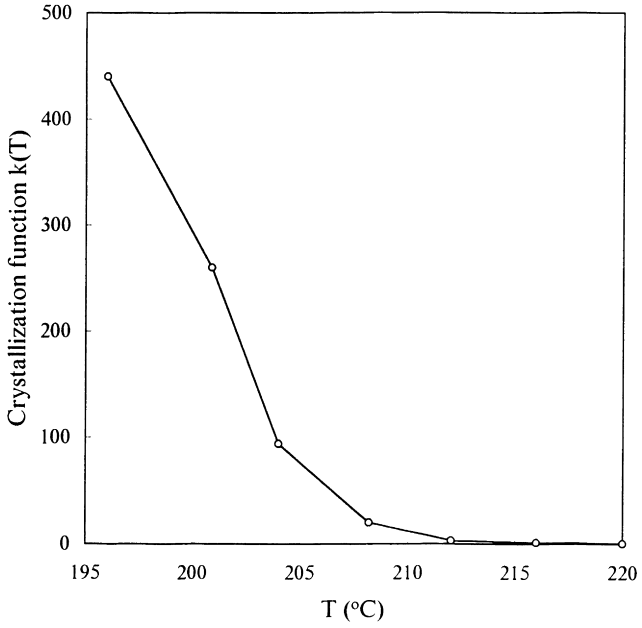

Fig. 6. Dependence of crystallization growth function k on temperature for non-isothermal crystallization of PBN. k values obtained using the Ozawa approach.

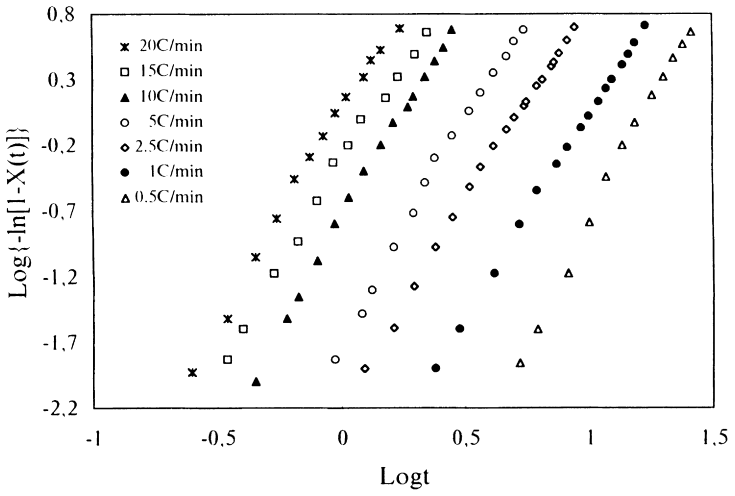

Fig. 7. Avrami plots for non-isothermal crystallization of PBN.

exponential dependence of the growth function k on T is shown in Fig. 6.

3.2.2. Avrami analysis of non-isothermal crystallization

The Avrami equation can be modified in order to describe non-isothermal crystallization [13–17]. For non-isothermal crystallization at a chosen cooling rate, the relative crystallinity $X(t)$ is a function of temperature. The crystallization temperature can be converted into crystallization time t using the equation

$$t = (T_o - T)/\alpha$$

where α is the cooling rate and T_o is the onset temperature of crystallization.

The Avrami parameters can be estimated from the $\log\{-\ln[1 - X(t)]\}$ vs $\log t$. The rate of non-isothermal crystallization depends on the cooling rate. Assuming a constant cooling rate, the crystallization rate constant can be corrected as follows [13]:

$$\log k' = (\log k)/\alpha.$$

The crystallization half time $t_{1/2}$ can be calculated from the corrected crystallization constant k' using the equation

$$t_{1/2} = (\ln 2/k')^{1/n}.$$

It is seen in Fig. 7, that two regimes in crystallization exist, since the slope of the $\log\{-\ln[1 - X(t)]\}$ vs $\log t$ changes. In the first regime, the slope is greater than that of the second regime. The retardation of crystallization should be attributed to the secondary crystallization.

In general, the modified-Avrami equation is valid only for the first regime in which the primary crystallization occurs. So, for each cooling run the Avrami parameters were estimated from the slope and intercept of the plot at the first regime. The Avrami exponent was found to be from 3.2 up to 4.4. Values for the exponent decrease as the cooling rate increases, or in other words as the supercooling increases (Table 3).

Values of the Avrami exponent are relatively larger than

Table 3
Results of the Avrami analysis for non-isothermal crystallization

Cooling rate (°C/min)	Avrami exponent n	log k	Crystallization half time $t_{1/2}$[a] (min)	Crystallization half time $t_{1/2}$[b] (min)
0.5	4.40	−3.50000	35.87	15
1	3.51	−2.90000	5.68	12.50
2.5	3.24	−0.91000	1.69	4.20
5	3.46	−0.34600	1.49	2.70
10	3.38	−0.07200	1.11	1.40
15	3.28	−0.01730	1.07	1.00
20	3.20	0.000540	0.83	0.85

[a] Values calculated from k'.
[b] Values calculated directly from the relative crystallinity vs time plot.

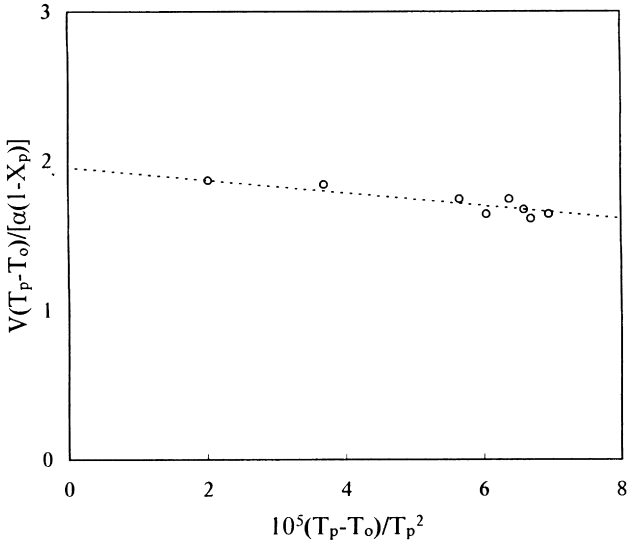

Fig. 8. Relationship between $V(T_p - T_o)/[\alpha(1 - X_p)]$ and $(T_p - T_o)/T_p^2$ for non-isothermal crystallization of PBN at various cooling rates.

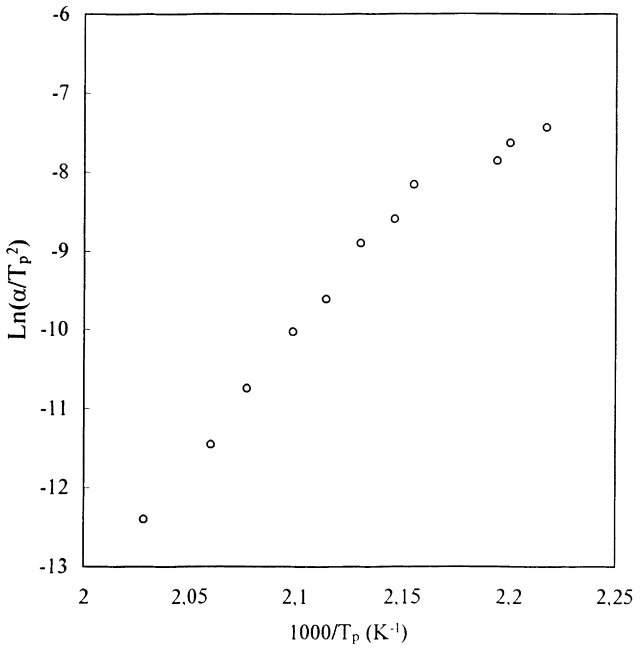

Fig. 9. Ln (α/T_p^2) vs $1/T_p$ plot according to the Kissinger method.

those found by the Ozawa analysis. This has been also, reported for other polymers.

The crystallization constant k increases with increasing cooling rate, while the crystallization half time decreases. This was expected since both k (or k') and $1/t_{1/2}$ are measures of the crystallization rate which get faster with supercooling.

Gupta et al. [22] for the description of non-isothermal crystallization modified the Avrami equation in combination with the Arrhenius equation:

$$k = A\exp(-E/RT)$$

where A is the preexponential factor and E is the activation energy of the crystallization process.

By derivation of the Avrami equation it follows for the rate equation for isothermal crystallization

$$V = dX/dt = nk^{(n-1)}(1 - X).$$

For crystallization during constant cooling with a cooling rate α, the temperature reduces as follows:

$$T = T_o - \alpha t$$

where T_o is the onset temperature of non-isothermal crystallization.

At peak crystallization maximum, the derivative of the rate equation should be equal to zero,

$$dX'/dt = 0.$$

After combinations of the above equations and reorganization it follows:

$$V(T_p - T_o)/[\alpha(1 - X_p)] = (n - 1) - E(T_p - T_o)/(RT_p^2)$$

where T_p is the peak temperature of non-isothermal crystallization.

From the last equation it follows that the plot of $V(T_p - T_o)/[\alpha(1 - X_p)]$ vs $(T_p - T_o)/(RT_p^2)$ would be a straight line with slope and intercept equal to E/R and $(n - 1)$, respectively. The corresponding plot for PBN crystallized by cooling from the melt by 0.5 to 20°C/min can be seen in Fig. 8, from which n was found to be 2.9. The activation energy was found 9.5 kcal/mol.

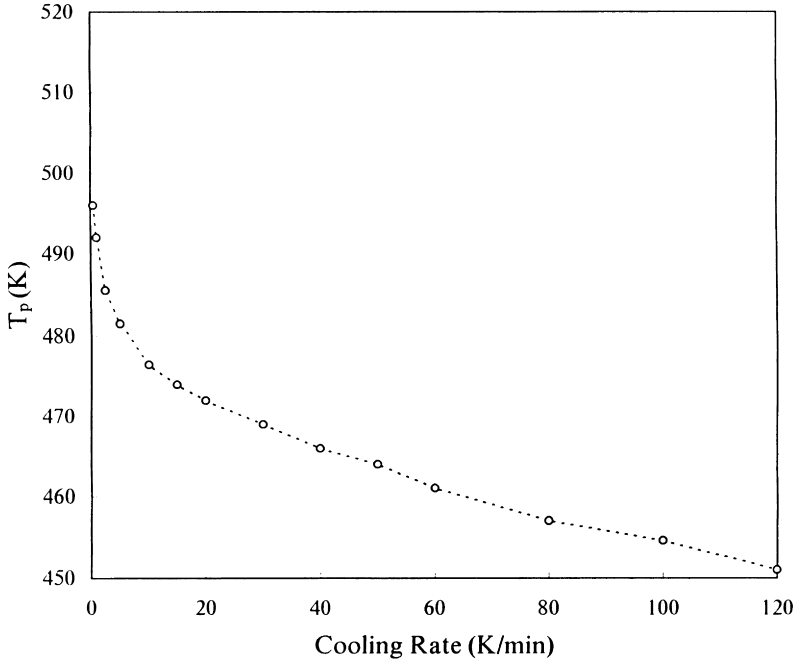

Fig. 10. Peak temperature vs cooling rate for non-isothermal crystallization of PBN.

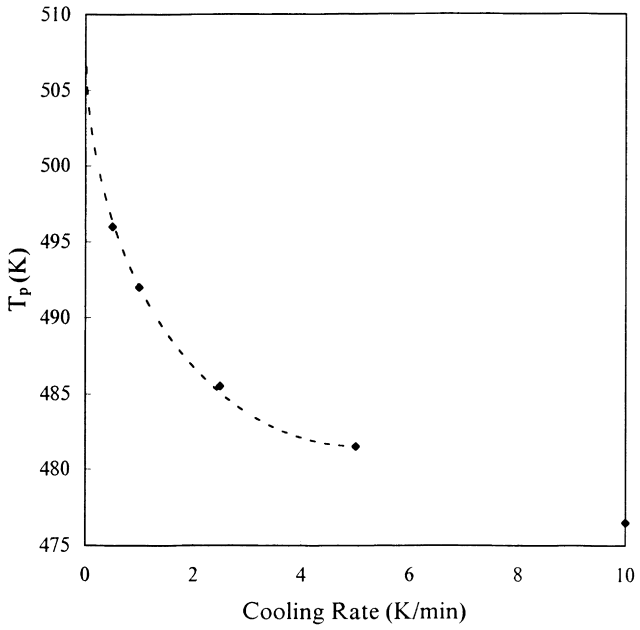

Fig. 11. Estimation of the ultimate crystallization temperature for PBN.

For non-isothermal crystallization, the activation energy E_a, can be derived from the variation of the crystallization peak temperature T_p with the cooling rate α, by the Kissinger approach [29,30]:

$$d[\ln(\alpha/T_p^2)]/d(1/T_p) = -E_a/R$$

where R is the gas constant.

The Kissinger plot, that is the plot of α/T_p^2 vs $1/T_p$, for PBN as seen in Fig. 9, exhibits very good linearity. The calculated value for activation energy is 11.5 kcal/mol, that is very close to that calculated with the method of Gupta et al.

Khanna [31] introduced a 'crystallization rate coefficient' (CRC) defined as the variation in cooling rate required to change the undercooling of the polymer melt of 1°C. The CRC can be measured from the slope of the plot of cooling rate vs crystallization peak temperature. The CRC values are higher for faster crystallizing systems. In Fig. 10 the plot of crystallization peak vs cooling rate can be seen for PBN. From the plot in Fig. 11, where results for very slow cooling rates are shown, the crystallization temperature for zero cooling rate can also be estimated. This corresponds to the ultimate temperature at which crystallization can be achieved. For PBN this seems to be above 508 K or 235°C. By means of polarizing microscopy it was observed that even at 250°C first crystal nuclei in the PBN metastable melt were formed in less than half an hour, but crystal growth was too slow.

According to Zhang et al. [32,33] crystallization rates for different polymers can be compared by plotting the reciprocal of half time of crystallization, against the cooling rate. The corresponding plot for PBN can be seen in Fig. 12.

3.3. Melting of PBN

The equilibrium melting point of PBN, calculated using the Hoffman–Weeks approach, was reported to be 294°C [27,28]. In this work, the melting peak temperature for PBN at DSC traces was found to vary from 239°C, for rapidly cooled samples, up to 264°C for annealed samples. However, using polarizing microcopy, the temperature at which crystals completely disappeared was found to be 262.5°C, for samples for which the melting peak temperature in the DSC traces was 248°C and the temperature at the end of the peak was 253°C.

As PBN has fast crystallization rates, metastable crystalline phases can be observed. Generally, double melting peaks were observed in DSC scans on heating, after isothermal crystallization. However, double melting peaks were also observed after non-isothermal crystallization by slow cooling rates, such as 0.5, 1, or 2.5°C/min (Fig. 13). In the latter case non-isothermal crystallization was found to take place at about 225–205°C. Since crystallization was very fast at T_cs lower than 220°C, slow cooling provided long enough time for crystallization to occur within a narrow temperature region, resulting in quite stable crystals. So that, the resulting morphology was similar to that produced by isothermal crystallization. The low melting peak is associated with melting secondary crystals, while the ultimate melting peak is associated with melting of primary crystals, as it was previously reported for PET, PEN and other polymers [34–45].

After isothermal crystallization at lower T_cs or fast cooling from the melt an exotherm attributed to recrystallization was observed, especially for slow heating rates, and only the ultimate melting peak can be observed [26,38,43].

Two models are usually elaborated for the treatment of the multiple melting of polymers. One assuming the overall process as a sequence of melting, recrystallization and final melting of the crystals and a second based on the concept of different crystal populations.

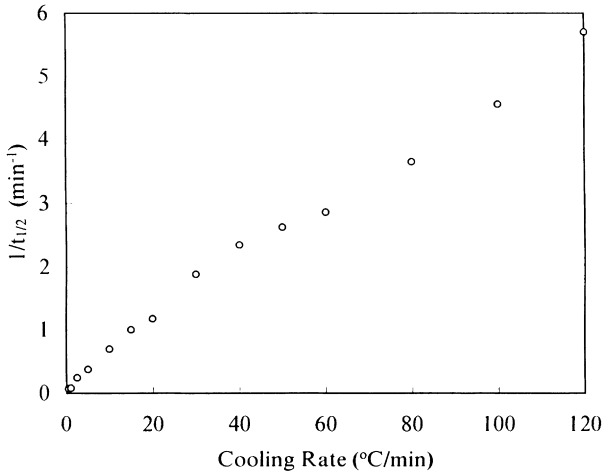

Fig. 12. $1/t_{1/2}$ vs cooling rate for non-isothermal crystallization of PBN.

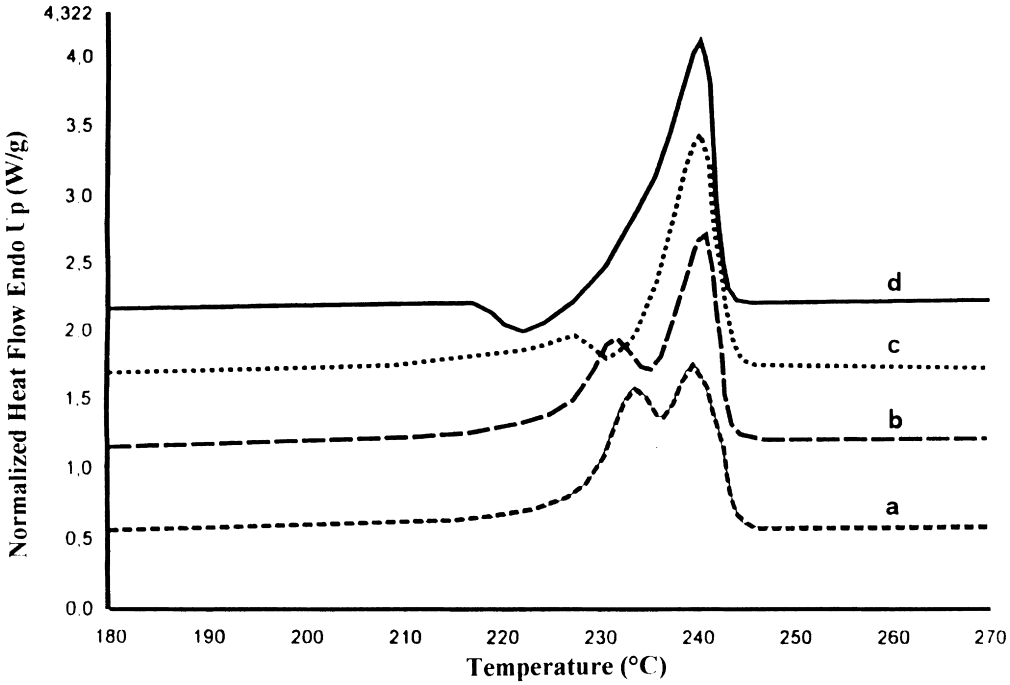

Fig. 13. DSC traces on heating at 20°C/min, for PBN cooled from the melt at various cooling rates: (a) 0.5°C/min; (b) 1°C/min; (c) 2.5°C/min; and (d) 10°C/min.

Since crystal nucleation for PBN was fast, especially below 220°C, a wide crystal size distribution was observed. During heating, small defective crystals melted first and this metastable melt recrystallized forming new crystals of increased stability. Since this initial melting occurred at low temperatures, recrystallization was expected. The driving force for crystallization, that is the supercooling, was large since the temperature of the metastable melt was low.

Small or secondary crystals, which were generated at a low temperature, are metastable crystalline phases. Polymer chains trapped in such metastable crystalline phases, after melting of these crystals of low stability, can gain the proper mobility to form crystalline phases of increased stability. This can happen since the melting occurred at temperatures low enough for the supercooling to be large, while at the same time these temperatures were high enough for the chains to gain proper mobility to form large stable crystals.

Besides, when the temperature increases beyond the $T_{\alpha,c}$, i.e. the temperature at which mobility of polymer segments within the crystal lattice starts, this motion results in quite an increase of the lamellar thickness. The latter case of

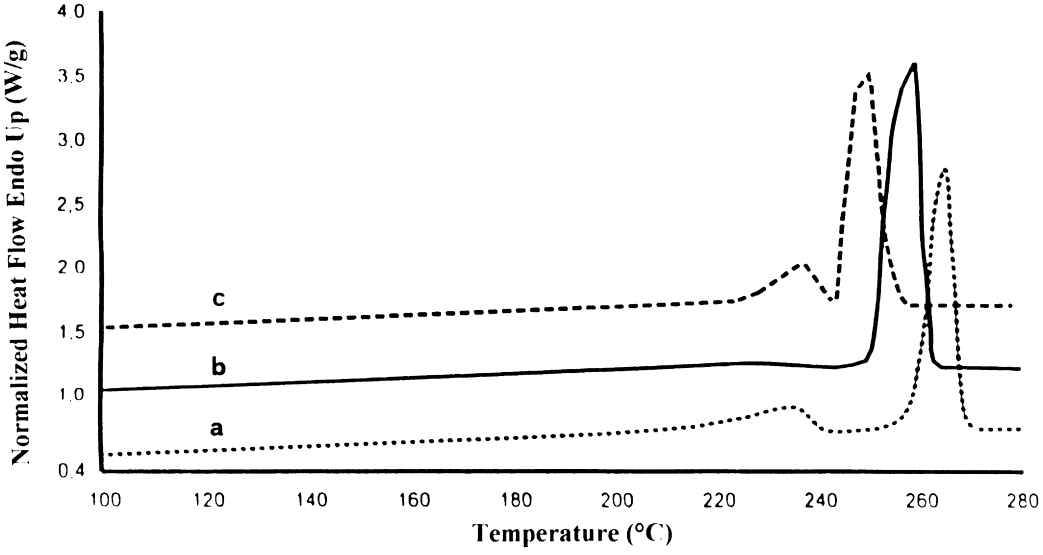

Fig. 14. DSC traces on heating at 20°C/min for PBN annealed at: (a) 244°C for 5.5 h; (b) 236°C for 4.5 h; and (c) 232°C for 3.5 h.

annealing and crystal perfection occurs in the solid state. Primary crystals with a significant stability, though they are not crystals of ultimate stability, can be perfected before their melting.

After annealing at elevated temperatures, the melting point of PBN was found to be increased. PBN, initially crystallized at moderate temperatures ($T_c = 212 - 225$°C), was heated at high temperatures, so that partial melting of even the stable crystals began. The melting temperature of PBN samples (original $T_m = 240 - 248$°C), after annealing at annealing temperatures 232–244°C for prolonged annealing times (3.5–5.5 h), was found to increase up to 264.5°C.

In fact, annealing at 232°C for 3.5 h of a sample crystallized initially at 213°C, with an original melting point 240°C, increased the melting temperature to 249°C, while the melting temperature of a sample after annealing at 236°C for 4.5 h increased from 248 to 258°C. Finally, after annealing a sample with an original melting point 248°C, at 244°C for 5.5 h, the melting point increased to 264.5°C (Fig. 14). The increase in the melting point verified the increased lamellar thickness and crystal perfection.

It must be noted that the material melted during heating to the annealing temperature did not crystallize again during the annealing, but it crystallized during cooling to the room temperature. A crystallization exotherm was observed at about 165–145°C during cooling by 150°C/min to the room temperature. So, a second, lower temperature, melting peak was observed corresponding to the melting of the crystal population formed during cooling to room temperature.

References

[1] Di Lorenzo ML, Silvestre C. Prog Polym Sci 1999;24:917.
[2] Avrami MJ. J Chem Phys 1939;7:1103.
[3] Avrami MJ. J Chem Phys 1940;8:812.
[4] Avrami MJ. J Chem Phys 1941;9:177.
[5] Kolmogorov AN. Bull Acad Sci USSR 1937;3:355.
[6] Johnson WA, Mehl RF. Trans Am Inst Miner Metall Pet Engng 1939;135:416.
[7] Kaschiev D, Sato K. J Chem Phys 1998;109:8530.
[8] Ozawa T. Polymer 1971;12:150.
[9] Nakamura K, Katayama K, Amano T. J Appl Polym Sci 1973;17:1013.
[10] Nakamura K, Watanabe T, Katayama K, Amano T. J Appl Polym Sci 1972;16:1077.
[11] Ziabicki A. Appl Polym Symp 1967;6:1.
[12] Ziabicki A, Sakjiewitz A. Colloid Polym Sci 1998;276:680.
[13] Jeziorny A. Polymer 1978;19:1142.
[14] Tobin MC. J Polym Sci, Polym Phys 1974;12:399.
[15] Cebe P, Hong SD. Polymer 1986;27:1183.
[16] De Juana R, Jauregui A, Calahora E, Cortazar M. Polymer 1996;37:3339.
[17] Cebe P. Polym Comp 1988;9:271.
[18] Lopez LC, Wilkes LG. Polymer 1989;30:882.
[19] Pena B, Delgado JA, Bello A, Perez E. Polymer 1994;35:3039.
[20] De Juana R, Jauregui A, Calahora E, Cortazar M. Polymer 1996;37:3339.
[21] Addonizio ML, Martuscelli E, Silvestre C. Polymer 1987;28:183.
[22] Gupta AK, Rana SK, Deopura B. J Appl Polym Sci 1994;51:231.
[23] Patel RM, Bheda JH, Spruiell J. J Appl Polym Sci 1991;42:1671.
[24] Hieber CA. Polymer 1995;36:1455.
[25] Yamanobe T, Matsuda H, Imai K, Hirata A, Mori S, Komoto T. Polym J 1996;28:177.
[26] Papageorgiou GZ, Karayannidis GP. Polymer 1999;40:5325.
[27] Karayannidis GP, Papageorgiou GZ, Bikiaris DN, Tourasanidis EV. Polymer 1998;39:4129.
[28] Lee SC, Yoon KH, Kim JH. J Appl Polym Sci 1997;29:1.
[29] Kissinger HE. J Res Natl Bur Stds (US) 1956;57:217.
[30] Kissinger HE. Anal Chem 1957;29:1702.
[31] Khanna P. Polym Engng Sci 1990;30:1615.
[32] Zhang R, Zheng H, Lou X, Ma D. J Appl Polym Sci 1994;51:51.
[33] Lee SW, Lee B, Ree M. Macromol Chem Phys 2000;201:453.
[34] Medellin-Rodriguez FJ, Philips PJ, Lin JS, Avila-Orta CA. J Polym Sci, Polym Phys 1998;36:763.
[35] Yagpharov M. J Therm Anal 1986;31:1073.
[36] Blundell DJ. Polymer 1987;28:2248.
[37] Ko TY, Woo EM. Polymer 1996;37:1167.
[38] Kim HG, Robertson RE. J Polym Sci, Polym Phys 1998;36:1757.
[39] Cheng SZD, Wunderlich B. Macromolecules 1987;20:2802.
[40] Hobbs SY, Pratt CF. Polymer 1975;16:462.
[41] Alizadeh A, Richardson L, Xu J, Marand H, Cheung W, Chum S. Macromolecules 1999;32:6221.
[42] Qiu G, Tang ZL, Huang NX, Gerking L. J Appl Polym Sci 1998;69:729.
[43] Sauer BB, Kampert WG, Blanchard EN, Threefoot SA, Hsiao BS. Polymer 2000;41:1099.
[44] Hsiao BS, Gardner KH, Wu DQ, Chu B. Polymer 1993;34:3986.
[45] Wang ZG, Hsiao BS, Sauer BB, Kampert WG. Polymer 1999;40:4615.